International Journal on Recent and Innovation Trends in Computing and Communication
ISSN: 2321-8169 Volume: 11 Issue: 5
DOI: https://doi.org/10.17762/ijritcc.v11i5.6605
***Article Received**: 26 February 2023 **Revised**: 02 April 2023 **Accepted**: 20 April 2023*

Performance Evaluation of Hybrid Precoder Design for Multi-User Massive MIMO Systems with Low-Resolution ADCs/DACs

Girish Kumar N G[1], Dr. M N Sree Ranga Raju[2]
[1]Department of Electronics and Telecommunication Engineering,
Bangalore Institute of Technology,
Visvesvaraya Technological University, Bangalore, India
e-mail: girishkumarng@bit-bangalore.edu.in
[2]Department of Electronics and Communication Engineering,
Bangalore Institute of Technology,
Visvesvaraya Technological University, Bangalore, India
e-mail: mnsrr@rediffmail.com

Abstract— This paper presents a comprehensive analysis and design of a hybrid precoding system tailored for mmWave multi-user massive MIMO systems in both downlink and uplink scenarios. The proposed system employs a two-stage precoding approach, incorporating UQ and NUQ techniques, along with low-resolution DACs in downlink and ADCs in uplink to address hardware limitations. The system considers Zero Forcing and Minimum Mean Square Error algorithms as digital precoding methods for the uplink scenario, while exploring the impact of different DAC resolutions on system performance. Extensive simulations reveal that the proposed system surpasses conventional analog beamforming methods, particularly in multi-user scenarios involving inter-user interference. In downlink, the system demonstrates a trade-off between SE and EE, achieving higher Energy Efficiency with NUQ. In uplink, NUQ and UQ converters exhibit similar performance trends regardless of the chosen combiner algorithm. The proposed system attains enhanced Spectral and Energy Efficiency while maintaining reduced complexity and overhead. The study significantly contributes to the advancement of efficient and effective mmWave multi-user massive MIMO systems by providing a thorough analysis of various quantization schemes and precoding techniques. The findings of this research are expected to aid in the optimization of 5G and beyond technologies, particularly in high-density deployment scenarios.

Keywords- Multi User Massive MIMO, Uniform Quantization, Non-Uniform Quantization, Spectral Efficiency, Energy Efficiency, ADC, DAC, Zero Forcing, MMSE.

ABBRIVATONS

NOMENCLATURE			
$\boldsymbol{A}$	Analog Precoder Matrix	$\boldsymbol{N_u}$	Number of users
$\boldsymbol{D}$	Digital Precoder Matrix	$\boldsymbol{N_t}$	Total number of Transmit antennas
$\mathbf{N_t^{RF}}$	Number of RF chains at the Base Station	$\boldsymbol{N_r}$	Total number of receive antennas
$\mathbf{N_r^{RF}}$	Number of RF chains at the user	$\boldsymbol{N_{R_u}}$	Number of receive antennas at each user
$\boldsymbol{W}$	Overall Precoder Matrix	$\boldsymbol{N_m}$	Number of Data streams
$\boldsymbol{\Phi_{bs}}$	DAC Distortion	$\boldsymbol{m}$	Signal vector
$\boldsymbol{\Phi_{\alpha}}$	ADC distortion matrix	**MUI**	Multi User Interference
SE	Spectral Efficiency	**UQ**	Uniform Quantization
EE	Energy Efficiency	**NUQ**	Non Uniform Quantization
CSI	Channel State Information	**BPCU**	Bits Per Channel Usage
ZF	Zero Forcing	**MMSE**	Minimum Mean Square Error

I. INTRODUCTION

The deployment of massive multiple-input multiple-output (MIMO) [1] has become increasingly popular in cellular communication systems due to its significant improvements in both coverage and SE by using large-scale antenna arrays at the base station (BS) [1]. However, practical implementation of massive MIMO with very large antenna elements can cause excessive energy consumption and complicate the hardware and radio frequency (RF) circuit architectures of the BS [1]. To address these challenges, researchers have proposed the use of low-resolution digital-to-analog converters (DACs) and analog-to-digital converters (ADCs) [2], as they can significantly reduce the energy consumption of the BS and simplify hardware and RF circuit architectures. However, the use of

International Journal on Recent and Innovation Trends in Computing and Communication
ISSN: 2321-8169 Volume: 11 Issue: 5
DOI: https://doi.org/10.17762/ijritcc.v11i5.6605
***Article Received**: 26 February 2023 **Revised**: 02 April 2023 **Accepted**: 20 April 2023*

low-resolution quantizer's results in significant quantization error and inter-user interference in the downlink MIMO transmission, which limits the SE gains in massive MIMO [2].

In recent literature, researchers have proposed several solutions to address these challenges. A low-resolution quantized precoding algorithm that maximizes the EE of massive MIMO systems has been presented in [3]. In [4], a low-complexity hybrid precoding technique using a uniform linear array with low-resolution phase shifters was proposed. In [5], a hybrid precoding scheme that optimizes the trade-off between SE and EE in massive MIMO systems using low-resolution DACs was presented.

In this paper, we propose a novel hybrid precoding scheme for multi-user mmWave massive MIMO systems using low-resolution DACs. We investigate the impact of UQ and NUQ on the system's performance and compare it with other state-of-the-art hybrid precoding schemes. We also examine the impact of various system parameters, such as the number of antennas, the number of quantization bits, and the modulation scheme, on the system's performance. Designing efficient and effective massive MIMO systems is critical in modern cellular communication, and this research presents valuable contributions to the field.

II.LITERATURE SURVEY

In this paper, we present an extensive literature survey on the performance evaluation of hybrid precoder designs for multi-user massive MIMO systems incorporating low-resolution ADCs/DACs. Our goal is to thoroughly comprehend the current state-of-the-art, identify research gaps, and incorporate insights from our study to strengthen the body of work presented.

Numerous recent studies have investigated the impact of low-resolution ADCs/DACs on massive MIMO system performance. For example, Dai et al. [6] assess full-duplex massive MIMO systems with low-resolution ADCs/DACs and derive achievable rates considering quantization noise. Fan et al. [7] explore the influence of low-resolution ADCs on the spectral efficiency of massive MIMO systems, while Mo et al. [8] suggest near-optimal performance linear precoding methods. Jacobsson et al. [9] examine non-linear precoding schemes with one-bit ADCs/DACs. Despite these efforts, most existing literature does not investigate the potential advantages of NUQ methods in massive MIMO systems. Our work addresses this gap by analyzing the performance of massive MIMO systems employing NUQ techniques under various CSI conditions and evaluating the results for scenarios both with and without multi-user interference.

A growing number of publications have concentrated on developing and analyzing hybrid precoder designs for multi-user massive MIMO systems. For instance, Pavia et al. [18] propose low-complexity hybrid precoding designs for multiuser mmWave/THz ultra-massive MIMO systems, while Li et al. [19] explore 1-bit massive MIMO transmission, incorporating interference with symbol-level precoding. Zhang et al. [20] study the uplink cell-free massive MIMO system with mixed-ADC/DAC receivers, and Wang et al. [21] discuss the joint optimization of spectral and energy efficiency with low-precision ADCs in cell-free massive MIMO systems.

Our research proposes a novel hybrid precoder design for multi-user massive MIMO systems that utilizes both UQ and NUQ quantization. By considering hardware constraints and integrating a modified hybrid precoding technique based on Zero Forcing and Minimum Mean Square Error algorithms, we aim to improve system performance. Additionally, we examine the impact of perfect and imperfect CSI on multi-user interference. Our work differentiates itself by investigating the performance of massive MIMO systems using NUQ techniques under various CSI conditions and analyzing the results for cases with and without multi-user interference.

Regarding cell-free massive MIMO systems, Zhang et al. [22] probe secure transmission in the presence of RF impairments and low-resolution ADCs/DACs. Li et al. [23] analyze downlink performance in D2D underlaid multigroup multicast cell-free massive MIMO systems with low-resolution ADCs/DACs. Zhang et al. [24] focus on indoor THz communication systems with finite-bit DACs and ADCs, while Balti and Evans [25] explore full-duplex massive MIMO cellular networks with low-resolution ADC/DAC.Zhou et al. [26] study multigroup multicast downlink cell-free massive MIMO systems with multiantenna users and low-resolution ADCs/DACs. Kim et al. [27] investigate cell-free mmWave massive MIMO systems with low-capacity fronthaul links and low-resolution ADC/DACs. Choi et al. [29] propose energy efficiency maximization precoding for quantized massive MIMO systems.

Kwon et al. [31] discuss special issues on 6G and satellite communications. In [32], Wang et al. propose a joint hybrid precoding/combining scheme based on equivalent channels for massive MIMO systems. Liang et al. [33] investigate one-bit DACs precoding for massive MU-MIMO systems based on antenna selection architecture. Khalili et al. [34] propose receiver designs and communication strategies for MIMO networks with one-bit ADCs.

Emenonye et al. [35] explore differential modulation in massive MIMO with low-resolution ADCs. Osama et al. [36] provide a review on precoding techniques for mm-wave massive MIMO wireless systems. Wen et al. [37] investigate one-bit downlink precoding for massive MIMO OFDM systems. Finally, Zhang et al. [38] discuss achievable rates and allocation of quantization bits in massive MIMO systems with low-resolution ADCs.

International Journal on Recent and Innovation Trends in Computing and Communication
ISSN: 2321-8169 Volume: 11 Issue: 5
DOI: https://doi.org/10.17762/ijritcc.v11i5.6605
***Article Received**: 26 February 2023 **Revised**: 02 April 2023 **Accepted**: 20 April 2023*

Our work contributes to the literature by proposing a novel hybrid precoder design for multi-user massive MIMO systems that employs both UQ and NUQ quantization. Our approach considers hardware constraints and integrates a modified hybrid precoding technique based on Zero Forcing and Minimum Mean Square Error algorithms to enhance system performance. Furthermore, we scrutinize the impact of perfect and imperfect CSI on multi-user interference. Our research distinguishes itself by investigating the performance of massive MIMO systems using NUQ techniques under various CSI conditions and analyzing the results for cases with and without multi-user interference.

In conclusion, this literature survey offers a comprehensive overview of the state-of-the-art in hybrid precoder design for multi-user massive MIMO systems with low-resolution ADCs/DACs. By proposing a novel hybrid precoder design that utilizes both UQ and NUQ quantization, we aim to significantly advance the development of efficient and effective mmWave multi-user massive MIMO systems.

III. CONTRIBUTIONS

In this study, we present several substantial advancements to fortify the research

- Develop a novel hybrid precoder design specifically tailored for mmWave Massive MIMO systems, incorporating both uniform (UQ) and non-uniform quantization (NUQ) methods in low-resolution DACs to cater to distinct system requirements and constraints.
- Thoroughly assess the proposed design by predicting its output across multiple performance metrics, such as spectral efficiency (SE) versus energy efficiency (EE), SE in relation to signal-to-noise ratio (SNR), SE as a function of the number of base station antennas, and power consumption concerning the number of base station antennas.
- Demonstrate the versatility of the hybrid precoder, which effectively balances system performance and hardware complexity by utilizing both UQ and NUQ techniques to optimize for higher precision, reduced feedback overhead, decreased power consumption, and increased SE.
- Provide a comprehensive analysis showcasing the superior performance of the proposed design in comparison to conventional schemes, revealing the benefits of NUQ for achieving higher SE at lower SNR levels and the advantages of UQ at higher SNR levels.
- Establish the proposed hybrid precoder design as a promising candidate for next-generation wireless communication systems, achieving high SE and EE with low power consumption, thus paving the way for more efficient and effective mmWave multi-user massive MIMO systems.

IV. SYSTEM OVERVIEW

A. *System Model*

This section provides an overview of the Multiuser massive MIMO system under consideration in this work. The system comprises N_t transmitter antennas at the base station and N_u number of users with k receiver antennas. Figure 1 depicts the system, where each of the N_t transmitter antennas is connected to a distinct RF chain, and N_m streams of data symbols, represented by a vector m, are transmitted through an array of N_t transmitter antennas. The user data is scrambled, encoded, and modulated.

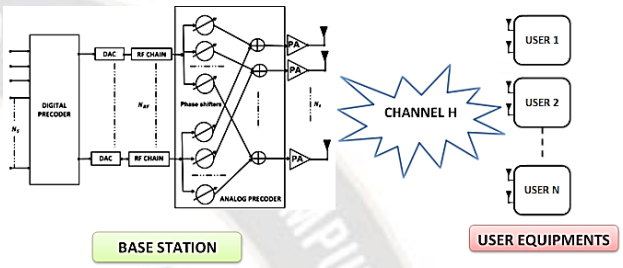

Figure. 1 Multi User Massive MIMO System

The modulated data undergoes digital precoding using an $N_t^{RF} \times N_m$ digital precoder, where N_t^{RF} is the number of RF chains at Base Station and N_m is the number of streams. Each of the N_t^{RF} streams is OFDM modulated, and the OFDM modulated symbols are converted to the analog domain using NUQ low-resolution DAC. The IFFT output is split into In-phase and Quadrature (I/Q) signals, and each I/Q signal is converted to equivalent analog data and modulated using an I/Q modulator. To maintain the desired amplitude of the symbols, a variable gain amplifier (VGA) is utilized to boost the I/Q symbols before up-conversion. The up-converted signal is passed through a bandpass filter (BPF) to limit the spectrum to the desired band and then amplified using a power amplifier (PA). The output of the PA is phase-shifted using a phase shifter and analog Precoded before being radiated into free-space. At the user end, each receiving antenna's input passes through a low-noise amplifier (LNA) to amplify the signal without adding noise and improve the SNR. The LNA's output is combined at the analog combiner stage, and the combined outputs are passed through the RF chain's bandpass filter before being down-converted and passed through I/Q demodulation. The resulting analog signal is then converted to digital using a low-resolution ADC. The digital I/Q is then OFDM demodulated (FFT), and the digital combiner, which is the inverse of the digital precoder, is applied to the output. The resulting signal is constellation de-mapped and decoded, and the decoder's output is descrambled to produce an estimated copy of the transmitted user data. The transmitted symbols are assumed to be independent and Gaussian distributed random variables with zero mean and unit variance. The digital

International Journal on Recent and Innovation Trends in Computing and Communication
ISSN: 2321-8169 Volume: 11 Issue: 5
DOI: https://doi.org/10.17762/ijritcc.v11i5.6605
***Article Received**: 26 February 2023 **Revised**: 02 April 2023 **Accepted**: 20 April 2023*

precoder produces a digital precoder matrix $D \in \mathbb{C}^{N_t{}^{RF} \times N_m}$, and the Precoded data is passed through a DAC before being processed by an analog precoder to generate an analog precoded matrix $A \in \mathbb{C}^{N_t \times N_t{}^{RF}}$. At the output of the transmitter, the transmitted vector $w \in \mathbb{C}^{N_t \times 1}$ is obtained by

$$w = \sqrt{P_t} A Q_D(.) Dm \tag{1}$$

The Quantizer function is represented by $Q_D(.)$ and the transmitted power is normalized to P_t. The transmitted vector experiences multipath fading due to channel imperfections. Assuming a narrowband fading channel with no intersymbol interference, the received vector $z \in \mathbb{C}^{N_T \times 1}$ is obtained after multipath fading and is given by,

$$z = Hw + n \tag{2}$$

Here, $H \in \mathbb{C}^{N_r \times N_t}$ represents the channel matrixcapturing a channel perturbations of a discrete Saleh-Valenzuela fading narrowband channel in which there is no mutual coupling and correlation between transmitter and receiver antennas is been considered and $n \in \mathrm{CN}(0, I_{N_T{}^{RF}})$ is the additive white gaussian noise. Since the received values go through ADC, before getting processed in the baseband, the received vector $r \in \mathbb{C}^{N_r \times 1}$ after ADC quantization can be given as:

$$r = Q_A(y) = Q_A(Hw + n) \tag{3}$$

$$\sigma_{lm}{}^2 = exp(-\gamma(T_l + \tau_{lm})) \tag{8}$$

At the transmitter side the symbols are converted to analog data by multiple DACs. After DAC processing a desired signal components are obtained by using Bussgang Theorem (Bussgang Theorem states that the cross correlation between any two Gaussian signals is same before and after one of them has passed through a non-linear function) which is given by:

$$t = Q_D(Dm) = FDm + g \tag{4}$$

Where $D = [\mathrm{D}_1 + \mathrm{D}_2 + \mathrm{D}_3 + \cdots + \mathrm{D}_{N_t{}^{RF}}]^T$ input signal of the quantizer and F is the DAC processing matrix which is given by $F = (1 - \Phi_{bs}) I_{N_{RF}}$ where ζ is the distortion factor of DACs and the uncorrelated Quantization error $g \in \mathbb{C}^{N_t{}^{RF} \times 1}$.Therefore using equation (1), (2) and (6) the signal after the DAC process is given by:

$$y = (1 - \Phi_{bs})\sqrt{P_t} HADm + \sqrt{P_t} HAg + n \tag{5}$$

At the receiver side, the signal detected is quantized by ADCs. Using the Additive Quantization Noise Model the quantizer output is calculated by:

$$r = Q_A(y) = (1 - \Phi_\alpha) y + e \tag{6}$$

where Φ_α is the distortion induced by ADC and $'e'$ is the distortion noise of order $N_R \times 1$. Substituting equation (1),(2),(5) into (6) we get,

$$\begin{aligned} r = {} & (1 - \Phi_\alpha)(1 - \Phi_{bs})\sqrt{P_t} HADm \\ & + (1 - \Phi_\alpha)\sqrt{P_t} HAg \\ & + (1 - \Phi_\alpha) n + e \end{aligned} \tag{7}$$

From equation (7), it can be seen that the received vector is linearly dependent on the choice of precoding matrices A and D. The matrix A is the $N_t \times N_t{}^{RF}$ dimension Analog precoding matrix, that capture the weights of phase shifters and the matrix D is the $N_t{}^{RF} \times N_m$ dimension digital precoding matrix that capture the weights of digital precoding.

B. Channel Model

In this work, we employ the Saleh-Valenzuela (S-V) channel model to generate the channel matrix H for our massive MIMO communication system. The S-V model characterizes the multipath propagation in the system by considering the effects of multiple clusters and rays within each cluster.

Let N_t be the number of transmit antennas, K be the number of receive antennas, L be the number of clusters, and M be the number of rays within each cluster. Further, let T denote the mean cluster arrival time interval, τ represent the mean ray arrival time interval, and γ be the power decay factor.

For each cluster l $(l = 1, 2, \ldots, L)$, the arrival time T_l is generated based on a Poisson distribution with mean T. Similarly, for each ray m $(m = 1, 2, \ldots, M)$ within cluster l, the arrival time τ_{lm} is generated based on a Poisson distribution with mean τ.

The complex gain α_{lm} of each ray m within cluster l is a complex Gaussian random variable with zero mean and variance $\sigma_{lm}{}^2$. The variance $\sigma_{lm}{}^2$ is given by:

The channel matrix H is an $N_t \times K$ matrix, where each element H_{mn} represents the channel gain between the nth transmit antenna and the mth receive antenna. H_mn can be computed as:

$$H_{mn} = \sum_{l=1}^{L} \sum_{k=1}^{K} (\alpha_{lm} e^{j2\pi(T_l + \tau_{lm})}) \tag{9}$$

This equation represents the channel gain between the N^{th} transmit antenna and the k^{th} receive antenna by summing up the complex gains of each ray m within each cluster l. The complex gains α_{lm} are multiplied by a complex exponential term to account for the phase shift induced by the arrival times of each cluster and ray.

V. UQ AND NUQ PROCESS FOR LOW RESOLUTION DAC/ADC

Quantization is the process of converting continuous-valued inputs into discrete outputs with a finite number of levels. While UQ is commonly used, it may not be the optimal choice for natural signals such as speech signals, as it can result in poor quality for infrequent large signals and noticeable truncation effects for frequent small amplitude signals. NUQ with Companding can significantly reduce distortion compared to UQ by using wider partition cells at high amplitude levels and narrower partition cells at lower

International Journal on Recent and Innovation Trends in Computing and Communication
ISSN: 2321-8169 Volume: 11 Issue: 5
DOI: https://doi.org/10.17762/ijritcc.v11i5.6605
***Article Received**: 26 February 2023 **Revised**: 02 April 2023 **Accepted**: 20 April 2023*

amplitude levels. NUQ can also allocate more bits to the more perceptually important parts of the signal, resulting in more accurate representation of those parts. In contrast, UQ allocates an equal number of bits to all parts of the signal, leading to poorer performance for signals with a wide dynamic range or non-uniform distribution of energy. In low-resolution ADCs/DACs, NUQ techniques can enhance the Spectral and EE Performance of Multi User Massive MIMO systems. The specific equation for NUQ using low-resolution ADC and DAC will depend on the specific quantization scheme used, as well as other factors such as input signal properties and hardware implementation.

The general equation for NUQ involves dividing the input signal into quantization intervals with non-uniform widths, which can be determined based on perceptual importance, signal statistics, or other optimization criteria. The quantized output can be expressed as $q(n) = Q(x(n))$, where $x(n)$ is the input signal, $q(n)$ is the quantized output, and $Q(.)$ is the NUQ function that maps the input signal to the quantization intervals. The quantization function can be implemented using lookup tables, polynomial approximations, or other methods. The specific equation for NUQ using low-resolution ADC and DAC depends on the quantization scheme used and other factors, such as input signal properties and hardware implementation.

This work proposes a customized NUQ equation that takes into account the exponential and/or logarithmic dependence of the quantized value on the unquantized value. The derived custom NUQ equation is

$$x_i{}^q = \left[\frac{x_i(2^q-1)}{(2^q-1)}\right] * sign(x_i) * \left[\frac{x_{max}-x_{min}}{2^q+1}\right] \quad (10)$$

Where $*$ is the round-off operator, x_{max} and x_{min} are the maximum and minimum values of user Precoded symbols, and $x_i{}^q$ represents quantized data. The effectiveness of NUQ in low-resolution ADCs/DACs can depend on various factors, such as the specific application, input signal nature, and quantization scheme used. Therefore, NUQ techniques should be carefully considered and evaluated through simulation and analysis in the context of low-resolution ADCs/DACs.

VI. HYBRID PRECODER DESIGN AND ANALYSIS OF SE AND EE FOR MULTI USER MASSIVE MIMO SYSTEM

This section delves into the computation of SE and EE for a Massive MIMO system that uses low-resolution quantized converters, and also discusses the iterative alternating minimization algorithm used for Hybrid Precoder Design. SE measures the amount of data that can be transmitted over a given bandwidth, and for low-resolution quantized converters, it can be expressed as the ratio of the achievable data rate to the total bandwidth, EE, on the other hand, measures the amount of information that can be transmitted per unit of energy consumed and can be defined as the ratio of the achievable data rate to the total power consumption. To achieve high SE and EE in such systems, the Hybrid Precoder design is critical. The Hybrid Precoder is responsible for mapping digital signals onto the analog domain, which is then transmitted through the antennas. The iterative alternating minimization algorithm is commonly used for Hybrid Precoder design, which optimizes the analog and digital Precoders iteratively. The algorithm aims to minimize the total Mean Squared Error (MSE) between the actual and desired signal while also taking into account the constraints imposed by the low-resolution quantized converters. The algorithm has been shown to be effective in achieving high SE and EE in Massive MIMO systems with low-resolution quantized converters.

A. Analysis of SE

SE for a Multi User Massive MIMO for some kth user is given by,

$$SE = R_k(A, D_k) = log_2(1 + SlNR)$$
$$= log_2\left(1_{Nr} + \frac{R^k_{mm}}{R_{II} + R^k_{\hat{g}\hat{g}} + R_{\hat{n}\hat{n}} + R^k_{ee}}\right) \quad (11)$$

The desired signal power R_{mm} which is a covariance matrix of the desired signal part of the received vector r is calculated by:

$$R^k_{mm} = \mathbb{E}[\hat{m}\hat{m}^H]$$
$$= \frac{P}{N_c}\Phi^H_\alpha \Phi_\alpha \Phi^H_{bs}\Phi_{bs} H_K A D_K D^H_K A^H H^H_K \quad (12)$$

As transmitted N_m data symbol $m = [m_1 + m_2 + m_3 + \cdots + m_{N_m}]^T$ are considered to be independent and Gaussian Distributed variable with zero mean and unit Variance,

The DAC Distortion noise power $R_{\hat{g}\hat{g}}$ which is a covariance matrix of DAC induced distortion Φ_{bs} and is given by:

Therefore the DAC Distortion Noise Power is given by:

$$R^k_{\hat{g}\hat{g}}$$
$$= \sum_{l=1}^{N_u} \frac{P}{N_m}\Phi^H_\alpha \Phi_\alpha (1$$
$$- \Phi^H_{bs})\Phi_{bs} H_k A diag(D_l D_l^H) A^H H^H_k \quad (13)$$

The White Gaussian Noise Power $R_{\hat{n}\hat{n}}$ is obtained by:

$$R_{\hat{n}\hat{n}} = \mathbb{E}[\hat{n}\hat{n}^H] = \Phi^H_\alpha \Phi_\alpha l_{N_r} \quad (14)$$

The ADC quantization noise power can be given as

International Journal on Recent and Innovation Trends in Computing and Communication
ISSN: 2321-8169 Volume: 11 Issue: 5
DOI: https://doi.org/10.17762/ijritcc.v11i5.6605
Article Received: 26 February 2023 Revised: 02 April 2023 Accepted: 20 April 2023

$$R_{\hat{e}\hat{e}} = \left(1_{N_r} - \Phi_\alpha\right)^H \Phi_\alpha diag\left(E(yy^H)\right)$$

$$R_{\hat{e}\hat{e}} = \frac{P}{N_m}\left(\mathrm{I}_{N_r} - \Phi_\alpha\right)^H \Phi_\alpha diag(\Phi_{bs}^H \Phi_{bs} \mathrm{HADD^H A^H H^H} + \left(1 - \Phi_{bs}^H\right)\Phi_{bs}\mathrm{HA}diag(\mathrm{DD^H})\mathrm{A^H H^H} + T_{N_T}) \quad (16)$$

Therefore,

$$\mathrm{R_{ee}^k} = \sum_{l=1}^{N_u} \frac{P}{N_m}\left(\mathrm{I}_{N_r} - \Phi_\alpha\right)^H \Phi_\alpha diag(\Phi_{bs}^H \Phi_{bs} \mathrm{H_k AD_l D_l^H A^H H_k^H} + \left(\mathrm{I}_{N_t} - \Phi_{bs}^H\right)\Phi_{bs}\mathrm{H_k A}diag\left(\mathrm{D_l D_l^H}\right)\mathrm{A_k^H H_k^H} + T_{N_T}) \quad (17)$$

$$\mathrm{R_{II}} = \sum_{l=1, l\neq k}^{k} \mathrm{R_{mm}^l} \quad (18)$$

Finally by Equation (12), Equation (13), Equation (14) and Equation (17) we get,

$$SE = \mathrm{R_k(A, D_k)} = \log_2\left(1_{Nr} + \mathrm{R_n^{-1} H_k AD_K D_k^H A^H H_k^H}\right) \quad (19)$$

Where, $R_n = \mathrm{R_{II}} + \mathrm{R_{\hat{g}\hat{g}}^k} + \mathrm{R_{\hat{n}\hat{n}}} + \mathrm{R_{ee}^k}$

B. Hybrid Precoder Design

Two kinds of scenarios exist. When perfect CSI is not available at the transmitter/receiver there exists Inter user Interference, when perfect CSI is available at transmitter and receiver then Inter-user interference can be avoided using precoding/beamforming.

In this section, the focus is on designing a hybrid precoder to maximize the SE of the massive MIMO system. Algorithm 1 describes a two-stage precoding design for multi-user MIMO systems with inter-user interference. The algorithm starts by initializing an $\widetilde{\mathrm{A}}$ matrix with random phases. In the first stage, the algorithm iterates over K users and obtains the optimal $\mathrm{W_{opt,k}}$ matrix by selecting the first N_s singular vectors of the channel matrix H for the kth user. In the second stage, for some integer value M, the algorithm fixes the $\tilde{A}$ matrix and calculates the digital precoder matrix $\widetilde{D_k}$ using $\widetilde{D_k} = \tilde{A}^H W_{opJ,k}$. Then, the hybrid precoder matrix F_k is obtained by multiplying $W_{opt,k}$ and $\widetilde{D_k}^H$. Next, the algorithm updates the analog Precoded matrix $\tilde{A}$ by setting its elements to $\mathrm{e}^{j\angle|F_k|_{m,n}}$, where $|F_k|_{m,n}$ is the magnitude of the elements of F_k. For each user k, the algorithm checks if the norm of the difference between the optimal W matrix and the product of A and D_k is less than a predefined threshold value. If the condition is satisfied, the algorithm sets A and D to $\tilde{A}$ and $\widetilde{D}$, respectively, and completes the algorithm. Otherwise, the algorithm sets k=1 and checks if it has reached K users. If K users have been processed, the algorithm terminates. Otherwise, it continues with the next user. In summary, the algorithm iteratively updates the hybrid precoder matrix $\tilde{A}$ and digital precoder matrix $\widetilde{D}$ to minimize the interference caused by multiple users, resulting in an optimal precoder design for the multi-user MIMO system.

Algorithm 1		**Two stage precoding design in case of multi-user MIMO with MUI**
1	**Initialize**	Construct $\widetilde{\mathrm{A}}$ with random phases
2	**While**	k ≤ N_u do
3		obtain $\mathrm{W_{opt,k}} = \mathrm{V_H}(:, 1: N_m)$
4		**for** $1 \leq m \leq M$ do ; For some integer value M
5		Fix $\tilde{A}$, calculate $\widetilde{D_k} = \tilde{A}^H W_{opt,k}$
6		$F_k = W_{opt,k}\widetilde{D_k}^H$
7		Fix $\widetilde{D_k}$, update $\left[\tilde{A}\right]_{m,n} = \mathrm{e}^{j\angle|F_k|_{m,n}}$
8		$\forall k \in [1, .. K]$, Check If $\|w_{opt,k} - AD_k\|_F^2 < \in$,
9		If yes,
		set k = k + 1, Set $A = \tilde{A}$ and $\mathrm{D} = \widetilde{D} = \frac{\sqrt{N_s}\widetilde{D}}{\|A\widetilde{D}\|_F^2}$ // algorithm is completed
10		else
		set k = 1
		if k == K
		break;
		else
		continue;
11	**end**	

International Journal on Recent and Innovation Trends in Computing and Communication
ISSN: 2321-8169 Volume: 11 Issue: 5
DOI: https://doi.org/10.17762/ijritcc.v11i5.6605
***Article Received**: 26 February 2023 **Revised**: 02 April 2023 **Accepted**: 20 April 2023*

Algorithm 2 describes a two-stage precoding design in the case of multi-user multiple-input multiple-output (MIMO) without inter-user interference. The algorithm is used to optimize the precoding matrices for each user in a multi-user MIMO system, with the goal of minimizing the overall transmit power required to achieve a desired quality of service. The algorithm begins by initializing a matrix A with random phases. Then, for each user k, the algorithm computes the singular value decomposition (SVD) of the channel matrix H_k, which is the MIMO channel between the transmitter and user k. Next, the algorithm initializes a matrix Z_k, which is an $(M \times N_s)$ matrix containing the singular vectors that are orthogonal to the ones used for the streams of user k. This matrix is used to construct the precoding matrix for user k. The algorithm then fixes the value of $\tilde{A}$ and calculates the product of the conjugate transpose of $\tilde{A}^H$ with the optimal weight vector for user k, denoted by $W_{opt,k}$, to obtain a new vector $\widetilde{D_k}$. Using $\widetilde{D_k}$, a precoding matrix is constructed for user k, denoted by F_k.

The value of $\widetilde{D_k}$ is fixed and the phase of $\tilde{A}$ is updated based on the magnitudes of the elements of F_k. This process is repeated for all users in the system, and the algorithm checks if the norm of the difference between the optimal weights vector and the product of $\tilde{A}$ and $\widetilde{D_k}$ is less than a certain threshold.

If the threshold is met, the algorithm increments k and repeats the process for the next user. If the threshold is not met, the algorithm resets k to 1 and repeats the process from the beginning. If all users have been processed and the threshold has been met for each user, the algorithm saves the values of A and D as the final precoding matrices and terminates. Overall, the algorithm 2 iteratively optimizes the precoding matrices for each user in the system until the transmit power is minimized and the desired quality of service is achieved.

Algorithm 2		**Two stage precoding design in case of multi-user MIMO without MUI**
1	**Initialize**	Construct $\widetilde{A}$ with random phases
2	**While**	k $\leq N_u$ do
3		Compute $U_h \sum_H V_H = \mathrm{SVD}(H_k)$
4		Initialize $(M \times N_m)$ matrix Z_k such that $V_H Z_k = [V_k^1 V_k^0]$ where V_k^0 is $N \times (N - N_{Ru})$ matrix containing singular vectors that are orthogonal to the ones used for the streams of user k.
5		Fix $\tilde{A}$, calculate $\widetilde{D_k} = \tilde{A}^H W_{opt,k}$
6		$F_k = W_{opt,k} \widetilde{D_k}^H$
7		Fix $\widetilde{D_k}$, update $[\tilde{A}]_{m,n} = e^{j\angle |F_k|_{m,n}}$
8		$\forall k \in [1,..K]$, Check If $\|w_{opt,k} - AD_k\|_F^2 < \in$,
9		If yes, Set $k = k + 1$ else set $k = 1$
10		if k == N_u Set $A = \tilde{A}$ and D = $\widehat{\mathrm{D}} = \frac{\sqrt{N_m}\widehat{\mathrm{D}}}{\|A\widehat{\mathrm{D}}\|_F^2}$ // algorithm is completed break; else continue;
11	**end**	

C. Analysis of EE

The Base station power consumption is given by,

$$P_{BS}(N_T, b_{DAC}, f_s, W) = P_{cir} + \kappa^{-1} P_{fx} = P_{tot} \quad (20)$$

P_{cir} is the circuit power consumption consisting of LO power, DAC power and RF front end power.

$$EE = \frac{B \times SE}{P_{tot}} \quad (21)$$

Where B is the Bandwidth of the system and SE is obtained in Equation (19).

TABLE 1 POWER CONSUMPTION BY EACH DEVICE

Device	**Notation**	**Values**
Local Oscillator	P_{LO}	22.5mW
Hybrid with buffer	P_{HB}	3mW
Power Amplifier	P_{PA}	P/0.25
Low Pass Filter	P_{LF}	14mW
Mixer	P_M	0.3mW
Phase Shifter	P_{PS}	21.6mW
RF Chain	P_{RF}	
DAC	P_{DAC}	Equation 30
ADC	P_{ADC}	

International Journal on Recent and Innovation Trends in Computing and Communication
ISSN: 2321-8169 Volume: 11 Issue: 5
DOI: https://doi.org/10.17762/ijritcc.v11i5.6605
Article Received: 26 February 2023 Revised: 02 April 2023 Accepted: 20 April 2023

$$P_{tot} = P_{LO} + P_{PA} + 2N_r P_{ADC} + N_{RF} N_t P_{ps} + N_{RF}(2P_{DAC} + P_{RF}) \quad (22)$$

$$P_{RF} = 2P_M + 2P_{LF} + P_{HB}, P_{DAC} = c_1 f_1 q + c_2 2^q \text{ and } P_{ADC} = j f_r 2^b \quad (23)$$

Where c_1 is a coefficient of Static Power Consumption = 9×10^{-12}, c_2 \$ is Dynamic Power Consumption = 1.5×10^{-5}, f_t is the sampling rate at transmitter, f_r is the sampling rate at receiver, q is the resolution of DACs, b is the resolution of ADCs and j is the consumption of energy per conversion step.

The EE maximization problem is formulated as

$$max \ \frac{R_k(A, D_k)}{P_{BS}(N, b_{DAC}, f_s, W)} AD_k \quad (24)$$

VII. SIMULATION RESULTS

The simulation results of a massive MIMO system with $N_t = 64, N_r = 4, k = 4, N_m = N_r{}^{RF} = 4$ as shown in the Figure 2 and Figure 3 reveal that varying the resolution 'q' of the DAC with $2, 4, and\ 6\ bits$ significantly impacts the system's SE versus SNR performance, with and without inter-user interference.

Figure. 2 illustrates the system's behaviour over an extensive range of SNR values, spanning from $-30\ dB\ to\ 60\ dB$, with SE values ranging between $0\ to\ 0.25\ BPCU$. As depicted in Figure. 2, the SE remains negligible at low SNR levels (from $-30\ dB$ to approximately $-15\ dB$) due to the dominance of noise and the adverse effects of multi-user interference, which significantly degrade the system's ability to accurately decode the transmitted symbols. However, as the SNR value surpasses $-10\ dB$, the SE demonstrates a gradual increase until it reaches $20\ dB$, as the received signal power becomes stronger relative to the noise power, mitigating the negative impact of interference, channel estimation errors, and quantization effects on system performance. Beyond $20\ dB$, the SE stabilizes and maintains a constant value, indicating that the system has reached its maximum capacity under the given conditions.

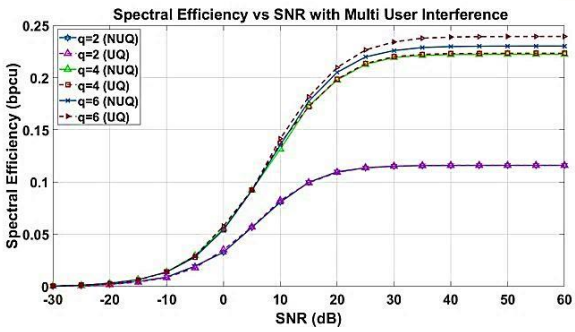

Figure 2. SE vs SNR with MUI when DAC Resolution 'q' is varied ($N_t = 64, N_r = 4, k = 4, N_s = N_t{}^{RF} = 4, q \in \{2,4,6\}$)

Figure. 3 illustrates the system's behaviour over an extensive range of SNR values with SE values ranging between $0\ to\ 1\ BPCU$. In the absence of multi-user interference, the performance improvement is more apparent, especially at low SNR levels. The SE still remains low at very low SNR values (from $-30\ dB$ to approximately $-15\ dB$) due to the dominance of noise. However, as the SNR value surpasses $-15\ dB$, the SE demonstrates a more pronounced increase, reaching a higher plateau compared to the scenario with multi-user interference. This improvement can be attributed to the fact that the system can now focus solely on mitigating noise, rather than dealing with both noise and interference. Beyond $20\ dB$, the SE stabilizes and maintains a constant value, indicating that the system has reached its maximum capacity under the given conditions without multi-user interference. Similar to the previous scenario, our analysis reveals that NUQ techniques exhibit superior performance for low-resolution DACs compared to their uniform counterparts.

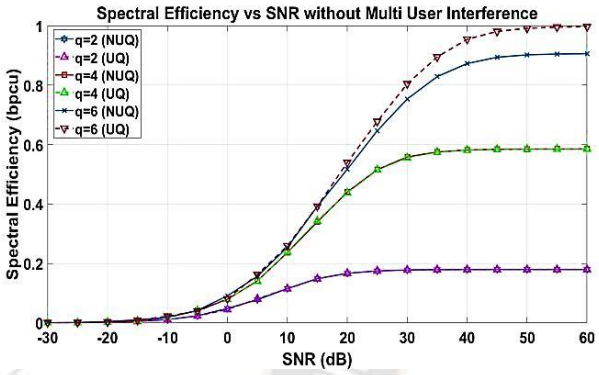

Figure 3. SE vs SNR without MUI when DAC Resolution 'q' is varied ($N_t = 64, N_r = 4, k = 4, N_s = N_t{}^{RF} = 4, q \in \{2,4,6\}$)

Figure. 4 illustrates the system's behaviour over an extensive range of SNR values, spanning from $-30\ dB\ to\ 60\ dB$, with SE values ranging between $0\ to\ 2\ BPCU$ in the presence of multi-user interference. In this case, the varying ADC resolution results in a more pronounced increase in SE, as higher ADC resolutions enable better signal representation and reduce the impact of quantization errors. Consequently, this leads to improved system performance even in the presence of multi-user interference.

International Journal on Recent and Innovation Trends in Computing and Communication
ISSN: 2321-8169 Volume: 11 Issue: 5
DOI: https://doi.org/10.17762/ijritcc.v11i5.6605
***Article Received**: 26 February 2023 **Revised**: 02 April 2023 **Accepted**: 20 April 2023*

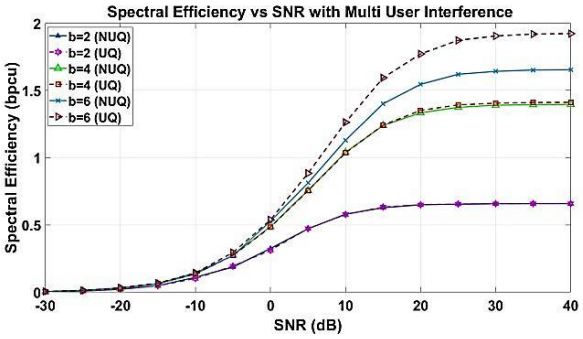

Figure 4. SE vs SNR with MUI when ADC Resolution 'b' is varied. ($N_t = 64, N_r = 4, k = 4, N_s = {N_r}^{RF} = 4, b \in \{2,4,6\}$)

Figure. 5 presents the same analysis for the scenario without multi-user interference. In this case, the SE values range between $0\ to\ 4.5\ BPCU$, demonstrating a substantial improvement in system performance. As the impact of multi-user interference is eliminated, the system can fully capitalize on the benefits offered by higher ADC resolutions, resulting in even higher SE values. The absence of interference allows the system to focus on mitigating noise, thereby achieving better overall performance. For both scenarios, our analysis reveals that NUQ exhibit superior performance compared to their uniform counterparts.

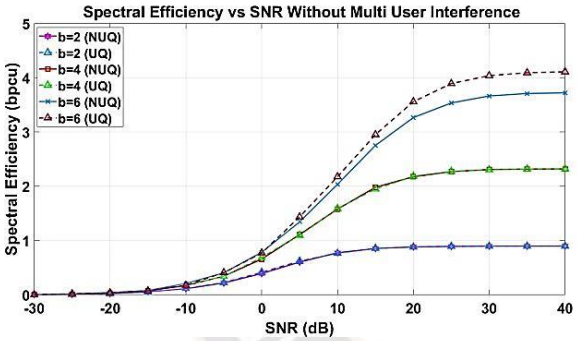

Figure 5. SE vs SNR without MUI when ADC Resolution 'b' is varied. ($N_t = 64, N_r = 4, k = 4, N_s = {N_r}^{RF} = 4, b \in \{2,4,6\}$)

Furthermore, NUQ can be more effective in reducing quantization noise in ADCs than UQ. NUQ allows more flexible allocation of quantization levels, which can result in a more efficient use of the available bits and a reduction in quantization noise. Overall, the simulation results suggest that varying the ADC resolution and considering NUQ can be a more effective way to improve the SE vs SNR performance of a massive MIMO system compared to varying the DAC resolution. However, the optimal choice of ADC resolution and quantization scheme may depend on various system parameters, and careful optimization is required to achieve the best possible performance.

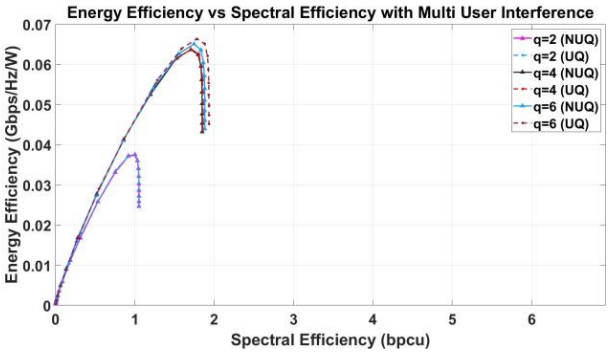

Figure 6. SE vs EE with MUI when DAC Resolution 'q' is varied ($N_t = 64, N_r = 4, k = 4, N_m = {N_t}^{RF} = 4, q \in \{2,4,6\}$)

Figure. 6 and Figure. 7 showcase the relationship between SE and EE for DAC resolution variation in the presence (Figure. 6) and absence (Figure. 7) of MUI. Our results indicate that increasing the DAC resolution leads to an increase in SE up to a certain point, after which it becomes almost constant, while the EE gradually decreases. This trade-off suggests that optimizing one metric comes at the cost of decreasing the other. We also observe that NUQ exhibits slightly lower performance compared to uniform UQ in the presence of MUI, attributable to the larger quantization errors for smaller values in NUQ.

Figure 7. SE vs EE without MUI when DAC Resolution 'q' is varied ($N_t = 64, N_r = 4, k = 4, N_m = {N_t}^{RF} = 4, q \in \{2,4,6\}$)

Figure. 8 and Figure. 9 examine the effect of ADC resolution variation on system performance under the same system parameters, with MUI (Figure. 8) and without MUI (Figure. 9). Our simulation results reveal that increasing the ADC resolution leads to improved SE and EE. However, the improvement is more pronounced in the absence of MUI, as the interference caused by other users is not present.

Both uniform and NUQ exhibit similar trends in SE and EE as the ADC resolution varies. The quantization error decreases with the increase in the number of bits used for quantization, leading to an improvement in SE. Nonetheless, this increase results in a decrease in EE, indicating a trade-off between the two metrics.

International Journal on Recent and Innovation Trends in Computing and Communication
ISSN: 2321-8169 Volume: 11 Issue: 5
DOI: https://doi.org/10.17762/ijritcc.v11i5.6605
***Article Received**: 26 February 2023 **Revised**: 02 April 2023 **Accepted**: 20 April 2023*

The observed discrepancy between the outcomes of SE vs SNR and SE vs EE plots upon varying ADC and DAC resolutions can be ascribed to the distinct roles that ADCs and DACs fulfil within the communication process and the specific metrics employed to assess system performance.

In the context of SE vs SNR plots, the emphasis lies on the system's capability to effectively decode and retrieve transmitted data amid noise, with SNR serving as the key parameter affecting the results. ADC resolution assumes a critical role in this regard, as it influences the received signal's representation, which can impact the precision of recovering transmitted information. Consequently, a more pronounced effect on SE vs SNR results is anticipated when varying ADC resolution.

Conversely, SE vs EE plots scrutinize the trade-off between the system's capacity to successfully transmit data and the energy expended during the process. DAC resolution impacts the transmitted signal's quality, which subsequently affects both SE and EE. Although elevated DAC resolutions can enhance SE, they also incur increased power consumption, leading to diminished EE. Therefore, the detected differences in SE vs EE plots upon varying DAC resolution correspond with the expected trade-offs between these performance metrics.

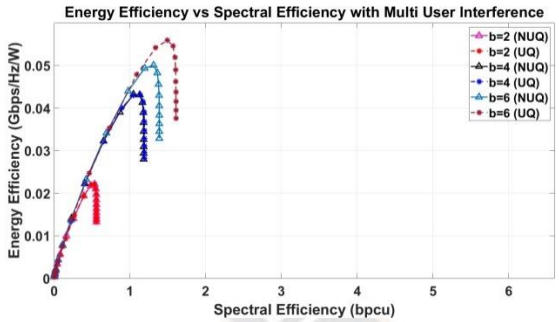

Figure 8. EE vs SE with MUI when ADC Resolution 'b' is varied. ($N_t = 64, N_r = 4, k = 4, N_m = {N_r}^{RF} = 4, b \in \{2,4,6\}$)

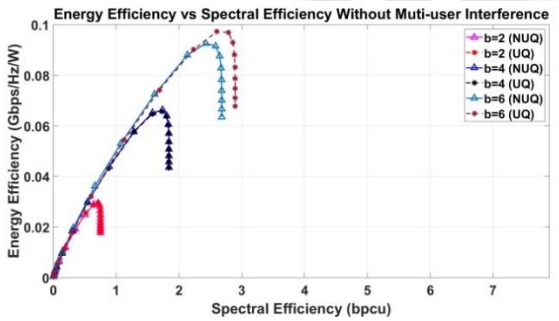

Figure 9. EE vs SE without MUI when ADC Resolution 'b' is varied. ($N_t = 64, N_r = 4, k = 4, N_m = {N_r}^{RF} = 4, b \in \{2,4,6\}$)

In conclusion, the divergent outcomes observed in SE vs SNR and SE vs EE plots upon varying ADC and DAC resolutions can be attributed to the unique roles of ADCs and DACs within the communication process and the particular performance metrics employed for system evaluation.

Figure 10 presents an analysis of the EE vs SE trade-off for a proposed hybrid preceded multi-user Massive MIMO system with low-resolution DACs (downlink) employing UQ and NUQ. The DAC resolutions under consideration include 2, 4, and 8 bits. The simulation results demonstrate that NUQ surpasses UQ in terms of EE, achieving an EE range of 0.75 bits/Joule to 1.88 bits/Joule, compared to UQ's 0.16 bits/Joule to 0.26 bits/Joule. In terms of SE, NUQ reaches 4.3 bits/sec/Hz to 11.3 bits/sec/Hz, while UQ attains 8.4 bits/sec/Hz to 11.5 bits/sec/Hz. These insights are crucial for optimizing massive MIMO systems' EE and SE, suggesting that employing a hybrid precoder with NUQ can enhance EE without sacrificing SE in comparison to UQ.

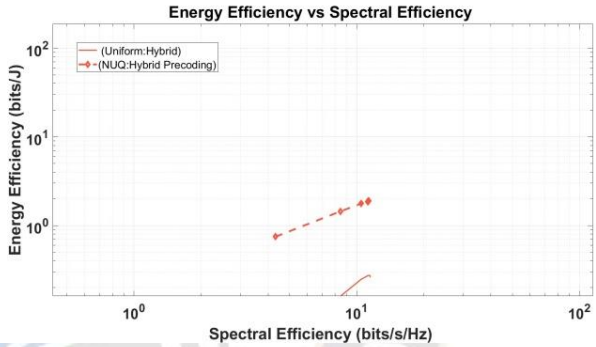

Figure 10. EE vs SE for a UQ and NUQ Converters (Downlink) ($N_t = 64, N_u = 1, k = 4, N_m = {N_r}^{RF} = 4, q = 16$)

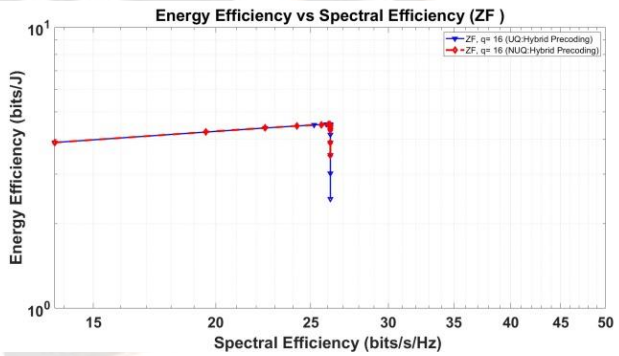

Figure 11. EE vs SE for a UQ and NUQ Converters (Uplink) when ZF combiner is considered($N_t = 64, N_u = 1, k = 4, N_m = {N_r}^{RF} = 4, q = 16$)

Figures 11 and 12 explore the EE vs SE trade-off in the uplink scenario for UQ and NUQ converters using ZF and MMSE detection. The results reveal that NUQ converters outperform UQ converters in terms of EE, with a range of 3.5 bits/Joule to 3.88 bits/Joule, while UQ converters display a range of 2.45 bits/Joule to 3.88 bits/Joule. Concurrently, the SE performance of NUQ converters spans from 13.64 bits/sec/Hz to 26.2 bits/sec/Hz, whereas that of UQ converters varies between 13.64 bits/sec/Hz and 26.2 bits/sec/Hz. Intriguingly, the trade-off curve remains consistent for both ZF and MMSE,

International Journal on Recent and Innovation Trends in Computing and Communication
ISSN: 2321-8169 Volume: 11 Issue: 5
DOI: https://doi.org/10.17762/ijritcc.v11i5.6605
***Article Received**: 26 February 2023 **Revised**: 02 April 2023 **Accepted**: 20 April 2023*

indicating that the choice of detection algorithm does not influence the EE vs SE performance. The performance disparity between downlink and uplink scenarios can be ascribed to the inherent differences in channel propagation characteristics and spatial correlation among users in these situations. In conclusion, the findings suggest that NUQ converters could constitute a promising solution for improving massive MIMO systems' EE in both downlink and uplink scenarios.

Figure 13 illustrates the relationship between power consumption and the number of base stations for UQ and NUQ converters in the downlink scenario, with varying DAC resolution 'q' (1, 3, 5, 7, and 16 bits). The results demonstrate an increase in power consumption as the number of base station antennas grows. Notably, a substantial gap in power consumption is initially observed between lower resolutions (q = 1, 3, 5, 7) and the highest resolution (q = 16); however, this gap diminishes as the number of base station antennas increases, with power consumption converging for both groups.

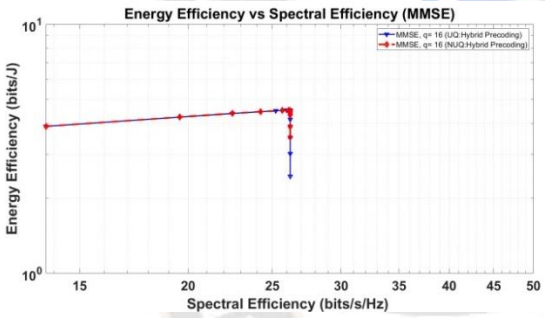

Figure 12. EE vs SE for a UQ and NUQ Converters (Uplink) when MMSE combiner is considered($N_t = 64, N_u = 1, k = 4, N_m = N_r{}^{RF} = 4, q = 16$)

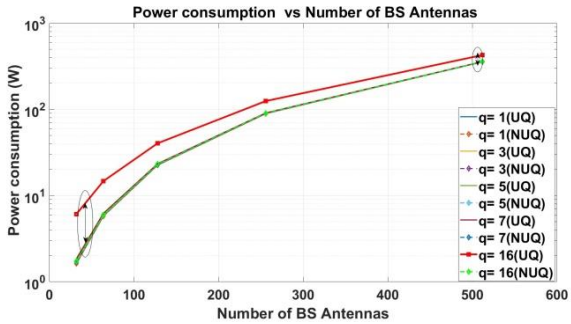

Figure 13. Power Consumption vs Number of Base Stations for a UQ and NUQ Converters with varied 'q' (Downlink)

This trend can be explained by the additional power requirements stemming from the increased number of base station antennas and the associated processing overhead. As the number of antennas rises, the impact of the added power consumption on the system surpasses the influence of DAC resolution, leading to a less pronounced difference in power consumption between lower and higher resolutions. These findings underscore the importance of considering both the number of base station antennas and the DAC resolution when optimizing power consumption in Massive MIMO systems.

Figure 14 and Figure 15 present the normalized power consumption versus the number of base station antennas for UQ and NUQ converters with varied 'q' (2, 4, 8 bits) in the uplink scenario, using ZF and MMSE combiners, respectively. The results for UQ and NUQ are compared with an optimum reference for each q value (2, 4, 8 bits). As the number of base station antennas increases from 50 to 500, the normalized power, expressed in dB, exhibits a decreasing trend, ranging from approximately 7 dB to around -8 dB for both UQ and NUQ.

The observed decrease in normalized power can be attributed to the enhanced spatial diversity and channel orthogonality as the number of base station antennas grows, allowing for improved power efficiency and reduced transmit power requirements for achieving the same SE. Negative dB values for normalized power signify that the actual transmit power required is less than the reference power, indicating higher power efficiency.

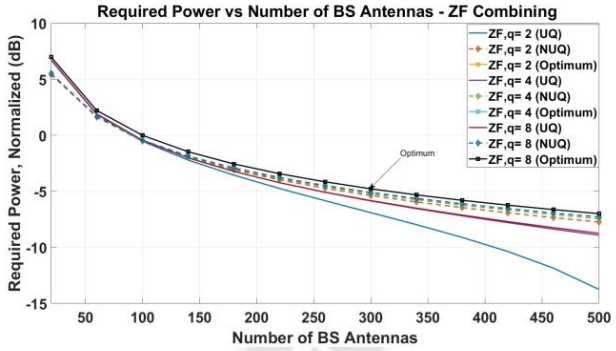

Figure 14. Power Consumption vs Number of Base Stations for a UQ and NUQ Converters with varied 'q' (Uplink) when ZF combiner is considered

Interestingly, the results show that the choice of combiner (ZF or MMSE) does not impact the normalized power consumption trends, suggesting that their interference cancellation capabilities are comparable under these conditions. Furthermore, the performance of both UQ and NUQ converters approaches the optimum results, indicating that these quantization methods can achieve near-optimal power efficiency in massive MIMO systems.

International Journal on Recent and Innovation Trends in Computing and Communication
ISSN: 2321-8169 Volume: 11 Issue: 5
DOI: https://doi.org/10.17762/ijritcc.v11i5.6605
***Article Received**: 26 February 2023 **Revised**: 02 April 2023 **Accepted**: 20 April 2023*

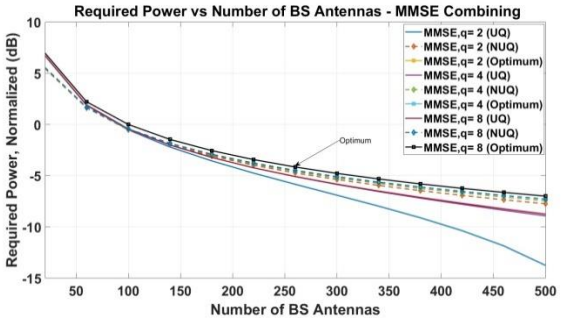

Figure 15. Power Consumption vs Number of Base Stations for a UQ and NUQ Converters with varied 'q' (Uplink) when MMSE combiner is considered

In conclusion, Figure 14 and Figure 15 highlight the potential for improved power efficiency in massive MIMO systems through antenna array expansion, with both UQ and NUQ converters exhibiting similar performance trends regardless of the chosen combiner algorithm.

Figure 16 presents a comparison of SE as a function of the number of base station antennas for UQ and non-uniform NUQ using low-resolution DACs with 2, 4, and 8 bits. The results highlight the differing performance trends between UQ and NUQ as the number of base station antennas increases. Specifically, UQ outperforms NUQ at lower numbers of base station antennas, while NUQ surpasses UQ when the number of antennas rises.

The enhanced performance of NUQ at higher SNRs can be attributed to its superior quantization of the received signal. As the number of antennas grows, NUQ leverages techniques such as beamforming to combine signals from each antenna and form a stronger signal in a specific direction. This process reduces noise and interference, leading to an elevated SNR.

Capitalizing on the increased SNR, NUQ employs a finer quantization scheme, which enables a more accurate representation of the received signal and fewer quantization errors. Consequently, this results in higher SE, representing the amount of data that can be transmitted per unit of bandwidth.

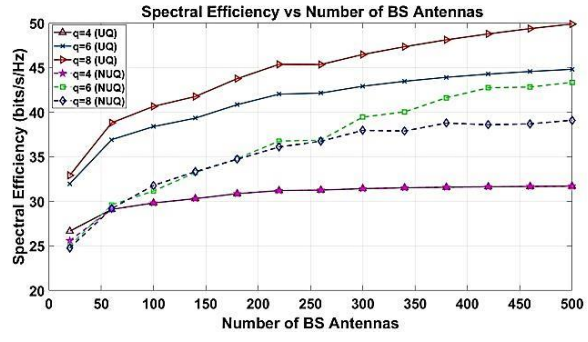

Figure 16. SE vs Number of Base Stations for a UQ and NUQ Converters with varied 'q' (Downlink)

Conversely, in scenarios with fewer base station antennas, the received signal is weaker and more susceptible to noise and interference. In such cases, UQ may be more effective due to its coarser quantization scheme, which is less sensitive to quantization errors.

Figure 17 and Figure 18 extend the analysis of SE as a function of the number of base station antennas to the uplink scenario, considering both ZF and MMSE combiners. These figures allow for a comprehensive evaluation of system performance in both downlink and uplink scenarios, as the uplink is an essential part of any communication system and must be optimized alongside the downlink for overall system performance.

In the uplink scenario, the results indicate a slight decrease in SE compared to the downlink, as illustrated in Figure 17 (ZF combiner) and Figure 18 (MMSE combiner). This reduction in SE can be attributed to the inherent differences in the uplink and downlink communication processes. The uplink is characterized by a higher degree of interference from multiple users transmitting data simultaneously towards the base station, as well as differences in channel propagation characteristics and spatial correlation between users.

UQ and NUQ exhibit similar trends in the uplink as observed in the downlink, with UQ outperforming NUQ at lower numbers of base station antennas and NUQ surpassing UQ as the number of antennas increases. The choice of combiner, either ZF or MMSE, does not significantly impact the SE performance in the uplink scenario, indicating that the choice of combiner is less critical in this context.

In conclusion, Figures 17 and Figure 18 provide valuable insights into the performance of massive MIMO systems in the uplink scenario, showcasing the importance of considering both uplink and downlink when optimizing system design. The results reveal the trade-offs between UQ and NUQ, as well as the implications of using combiners, highlighting the need to select the appropriate quantization scheme and combiner based on the specific scenario and system requirements.

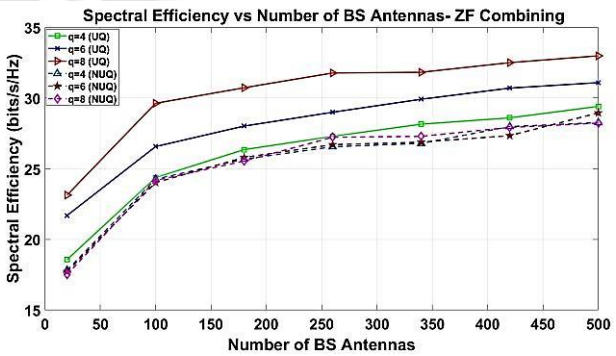

Figure 17. SE vs Number of Base Stations for a UQ and NUQ Converters with varied 'q' (Uplink) when ZF combiner is considered

International Journal on Recent and Innovation Trends in Computing and Communication
ISSN: 2321-8169 Volume: 11 Issue: 5
DOI: https://doi.org/10.17762/ijritcc.v11i5.6605
***Article Received**: 26 February 2023 **Revised**: 02 April 2023 **Accepted**: 20 April 2023*

In summary, this paper presents a comprehensive analysis of massive MIMO systems, investigating the trade-offs and performance metrics associated with different quantization schemes and combiner techniques in both downlink and uplink scenarios. Initially, we examined the impact of ADC resolution variation, which plays a critical role in the system's ability to recover transmitted data amid noise. However, we shifted our focus to DAC resolution variation when considering combiner techniques in uplink analysis. The rationale behind this decision is that DAC resolution has a more significant impact on the quality of the transmitted signal, which, in turn, affects both SE and EE, making it an essential parameter to analyse for massive MIMO systems.

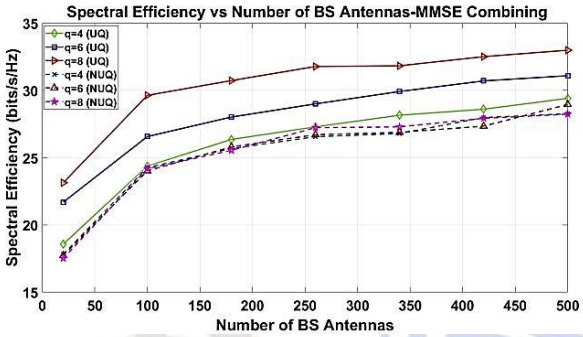

Figure 18. SE vs Number of Base Stations for a UQ and NUQ Converters with varied 'q' (Uplink) when MMSE combiner is considered

VIII.CONCLUSION

This paper has thoroughly analysed the performance of multi-user massive MIMO systems employing low-resolution ADCs and DACs with UQ and non-uniform NUQ techniques under various system parameters and scenarios. The objective of the study was to develop a comprehensive understanding of the trade-offs between SE and EE in multi-user massive MIMO systems while examining the influence of quantization techniques, detection algorithms, and the number of base station antennas on system performance.

A unique algorithm, based on the Saleh-Valenzuela channel model, was devised and employed to generate the channel matrix H for the considered multi-user massive MIMO systems. The algorithm capitalizes on the distinct characteristics of this model to allow for a more accurate representation of the wireless propagation environment.

The simulation results provided valuable insights into the performance trade-offs in multi-user massive MIMO systems. It was observed that NUQ could offer superior performance in terms of EE compared to UQ under certain conditions, such as higher SNR and a larger number of base station antennas. Furthermore, it was discovered that the choice of detection algorithm did not significantly impact the performance trends in terms of SE and EE.

These findings hold significant potential for optimizing the performance of multi-user massive MIMO systems in future 5G and beyond wireless communication networks. By carefully considering the system parameters, quantization techniques, and antenna configurations, it is possible to design communication systems that achieve a high level of efficiency while maintaining robust performance in terms of SE. The unique results presented in this paper contribute to the ongoing research in the field of multi-user massive MIMO and could serve as a foundation for further advancements in the area.

ACKNOWLEDGEMENT

I would like to thank Dr. SadaShivappa G, BOE, RVCE, Bangalore and Dr. Evan Jose, Research Dean, Christ University for their valuable guidance and support due to which we were able to successfully complete this research work.

REFERENCES

[1]. X. Liu *et al*., "Hybrid Precoding for Massive mmWave MIMO Systems," in *IEEE Access*, vol. 7, pp. 33577-33586, 2019, doi: 10.1109/ACCESS.2019.2903166.

[2]. J. Dai, J. Liu, J. Wang, J. Zhao, C. Cheng and J. -Y. Wang, "Achievable Rates for Full-Duplex Massive MIMO Systems With Low-Resolution ADCs/DACs," in IEEE Access, vol. 7, pp. 24343-24353, 2019, doi: 10.1109/ACCESS.2019.2900273.

[3]. J. Choi, J. Park and N. Lee, "Energy Efficiency Maximization Precoding for Quantized Massive MIMO Systems," in *IEEE Transactions on Wireless Communications*, vol. 21, no. 9, pp. 6803-6817, Sept. 2022, doi: 10.1109/TWC.2022.3152491.

[4]. F. Dong, W. Wang and Z. Wei, "Low-Complexity Hybrid Precoding for Multi-User MmWave Systems With Low-Resolution Phase Shifters," in *IEEE Transactions on Vehicular Technology*, vol. 68, no. 10, pp. 9774-9784, Oct. 2019, doi: 10.1109/TVT.2019.2933058.

[5]. Q. Ding, Y. Deng and X. Gao, "Spectral and Energy Efficiency of Hybrid Precoding for mmWave Massive MIMO With Low-Resolution ADCs/DACs," in *IEEE Access*, vol. 7, pp. 186529-186537, 2019, doi: 10.1109/ACCESS.2019.2959612.

[6]. Ding, Qingfeng, Yuqian Deng, and Xinpeng Gao. "Spectral and Energy Efficiency of Hybrid Precoding for mmWave Massive MIMO With Low Resolution ADCs/DACs." IEEE Access 7 (2019): 186529-186537.

[7]. X. Hu, C. Zhong, X. Chen, W. Xu, H. Lin and Z. Zhang, "Cell-Free Massive MIMO Systems With Low Resolution ADCs," in IEEE Transactions on Communications, vol. 67, no. 10, pp. 6844-6857, Oct. 2019, doi: 10.1109/TCOMM.2019.2927450

[8]. Y. Xiong, "Achievable Rates for Massive MIMO Relaying Systems With Variable-Bit ADCs/DACs," in IEEE Communications Letters, vol. 24, no. 5, pp. 991-994, May 2020, doi: 10.1109/LCOMM.2020.2971467.

International Journal on Recent and Innovation Trends in Computing and Communication
ISSN: 2321-8169 Volume: 11 Issue: 5
DOI: https://doi.org/10.17762/ijritcc.v11i5.6605
***Article Received**: 26 February 2023 **Revised**: 02 April 2023 **Accepted**: 20 April 2023*

[9]. Q. Ding, Y. Lian and Y. Jing, "Performance Analysis of Full-Duplex Massive MIMO Systems With Low-Resolution ADCs/DACs Over Rician Fading Channels," in *IEEE Transactions on Vehicular Technology*, vol. 69, no. 7, pp. 7389-7403, July 2020, doi: 10.1109/TVT.2020.2991143.

[10]. Q. Xu and P. Ren, "Secure Massive MIMO Downlink With Low-Resolution ADCs/DACs in the Presence of Active Eavesdropping," in IEEE Access, vol. 8, pp. 140981-140997, 2020, doi: 10.1109/ACCESS.2020.3013635.

[11]. S. J. Maeng, Y. Yapici, İ. Güvenç, H. Dai and A. Bhuyan, "Hybrid Precoding for mmWave Massive MIMO With One-Bit DAC," in IEEE Communications Letters, vol. 24, no. 12, pp. 2941-2945, Dec. 2020, doi: 10.1109/LCOMM.2020.3015674.

[12]. E. Vlachos and J. Thompson, "Energy-Efficiency Maximization of Hybrid Massive MIMO Precoding With Random-Resolution DACs via RF Selection," in IEEE Transactions on Wireless Communications, vol. 20, no. 2, pp. 1093-1104, Feb. 2021, doi: 10.1109/TWC.2020.3030772.

[13]. J. -C. Chen, "Spectral- and Energy-Efficient Hybrid Receivers for Millimeter-Wave Massive Multiuser MIMO Uplink Systems With Variable-Resolution ADCs," in IEEE Systems Journal, vol. 15, no. 2, pp. 1950-1958, June 2021, doi: 10.1109/JSYST.2020.2990753.

[14]. Zhou, M.; Zhang, Y.; Qiao, X.; Tan, W.; Yang, L. Analysis and Optimization for Downlink Cell-Free Massive MIMO System with Mixed DACs. Sensors 2021, 21, 2624. https://doi.org/10.3390/s21082624

[15]. L. Xu, C. Qian, F. Gao, W. Zhang and S. Ma, "Angular Domain Channel Estimation for mmWave Massive MIMO With One-Bit ADCs/DACs," in IEEE Transactions on Wireless Communications, vol. 20, no. 2, pp. 969-982, Feb. 2021, doi: 10.1109/TWC.2020.3029400.

[16]. S. -E. Hong, "Performance Analysis of Cell-Free mmWave Massive MIMO with Low-Resolution DAC Quantization," 2021 Twelfth International Conference on Ubiquitous and Future Networks (ICUFN), Jeju Island, Korea, Republic of, 2021, pp. 192-194, doi: 10.1109/ICUFN49451.2021.9528671.

[17]. Y. Xiong, S. Sun, N. Wei, L. Liu and Z. Zhang, "Performance Analysis of Massive MIMO Relay Systems With Variable-Resolution ADCs/DACs Over Spatially Correlated Channels," in IEEE Transactions on Vehicular Technology, vol. 70, no. 3, pp. 2619-2634, March 2021, doi: 10.1109/TVT.2021.3061699.

[18]. Pavia, J.P.; Velez, V.; Ferreira, R.; Souto, N.; Ribeiro, M.; Silva, J.; Dinis, R. Low Complexity Hybrid Precoding Designs for Multiuser mmWave/THz Ultra Massive MIMO Systems. *Sensors* 2021, *21*, 6054. https://doi.org/10.3390/s21186054

[19]. A. Li, C. Masouros, A. L. Swindlehurst and W. Yu, "1-Bit Massive MIMO Transmission: Embracing Interference with Symbol-Level Precoding," in *IEEE Communications Magazine*, vol. 59, no. 5, pp. 121-127, May 2021, doi: 10.1109/MCOM.001.2000601.

[20]. Y. Zhang, Y. Cheng, M. Zhou, L. Yang and H. Zhu, "Analysis of Uplink Cell-Free Massive MIMO System With Mixed-ADC/DAC Receiver," in *IEEE Systems Journal*, vol. 15, no. 4, pp. 5162-5173, Dec. 2021, doi: 10.1109/JSYST.2020.2999521.

[21]. Wang, H., Sun, C., Li, J. et al. Joint optimization of spectral efficiency and energy efficiency with low-precision ADCs in cell-free massive MIMO systems. Sci. China Inf. Sci. 65, 152301 (2022). https://doi.org/10.1007/s11432-021-3313-9.

[22]. X. Zhang, T. Liang, K. An, G. Zheng and S. Chatzinotas, "Secure Transmission in Cell-Free Massive MIMO With RF Impairments and Low-Resolution ADCs/DACs," in *IEEE Transactions on Vehicular Technology*, vol. 70, no. 9, pp. 8937-8949, Sept. 2021, doi: 10.1109/TVT.2021.3098693.

[23]. J. Li, A. Wan, M. Zhou, J. Yuan, R. Yin and L. Yang, "Downlink Analysis for the D2D Underlaid Multigroup Multicast Cell-Free Massive MIMO With Low-Resolution ADCs/DACs," in *IEEE Access*, vol. 10, pp. 115702-115715, 2022, doi: 10.1109/ACCESS.2022.3218721.

[24]. Y. Zhang, D. Li, D. Qiao and L. Zhang, "Analysis of Indoor THz Communication Systems With Finite-Bit DACs and ADCs," in *IEEE Transactions on Vehicular Technology*, vol. 71, no. 1, pp. 375-390, Jan. 2022, doi: 10.1109/TVT.2021.3123380.

[25]. E. Balti and B. L. Evans, "Full-Duplex Massive MIMO Cellular Networks with Low Resolution ADC/DAC," GLOBECOM 2022 - 2022 IEEE Global Communications Conference, Rio de Janeiro, Brazil, 2022, pp. 1649-1654, doi: 10.1109/GLOBECOM48099.2022.10001148.

[26]. M. Zhou, Y. Zhang, X. Qiao, M. Xie, L. Yang and H. Zhu, "Multigroup Multicast Downlink Cell-Free Massive MIMO Systems With Multiantenna Users and Low-Resolution ADCs/DACs," in *IEEE Systems Journal*, vol. 16, no. 3, pp. 3578-3589, Sept. 2022, doi: 10.1109/JSYST.2021.3077765.

[27]. I. -s. Kim, M. Bennis and J. Choi, "Cell-Free mmWave Massive MIMO Systems With Low-Capacity Fronthaul Links and Low-Resolution ADC/DACs," in *IEEE Transactions on Vehicular Technology*, vol. 71, no. 10, pp. 10512-10526, Oct. 2022, doi: 10.1109/TVT.2022.3184172.

[28]. Y. Zhang, D. Li, D. Qiao and L. Zhang, "Analysis of Indoor THz Communication Systems With Finite-Bit DACs and ADCs," in *IEEE Transactions on Vehicular Technology*, vol. 71, no. 1, pp. 375-390, Jan. 2022, doi: 10.1109/TVT.2021.3123380.

[29]. J. Choi, J. Park and N. Lee, "Energy Efficiency Maximization Precoding for Quantized Massive MIMO Systems," in IEEE Transactions on Wireless Communications, vol. 21, no. 9, pp. 6803-6817, Sept. 2022, doi: 10.1109/TWC.2022.3152491.

[30]. s. Kim, M. Bennis and J. Choi, "Cell-Free mmWave Massive MIMO Systems With Low-Capacity Fronthaul Links and Low-Resolution ADC/DACs," in IEEE Transactions on Vehicular Technology, vol. 71, no. 10, pp. 10512-10526, Oct. 2022, doi: 10.1109/TVT.2022.3184172.

International Journal on Recent and Innovation Trends in Computing and Communication
ISSN: 2321-8169 Volume: 11 Issue: 5
DOI: https://doi.org/10.17762/ijritcc.v11i5.6605
***Article Received**: 26 February 2023 **Revised**: 02 April 2023 **Accepted**: 20 April 2023*

[31]. Taesoo Kwon, Sooyoung Kim, Kyunghan Lee, Jong-Moon Chung, Special issue on 6G and satellite communications, ETRI Journal, 10.4218/etr2.12551, 44, 6, (881-884), (2022).

[32]. S. Wang et al., "A Joint Hybrid Precoding/Combining Scheme Based on Equivalent Channel for Massive MIMO Systems," in IEEE Journal on Selected Areas in Communications, vol. 40, no. 10, pp. 2882-2893, Oct. 2022, doi: 10.1109/JSAC.2022.3196099.

[33]. Rui Liang, Hui Li, Wenjie Zhang, Guodong Xue,One-bit DACs precoding for massive MU-MIMO systems based on antenna selection architecture, Digital Signal Processing, Volume 127, 2022, 103548, ISSN 1051-2004, https://doi.org/10.1016/j.dsp.2022.103548.

[34]. A. Khalili, F. Shirani, E. Erkip and Y. C. Eldar, "MIMO Networks With One-Bit ADCs: Receiver Design and Communication Strategies," in *IEEE Transactions on Communications*, vol. 70, no. 3, pp. 1580-1594, March 2022, doi: 10.1109/TCOMM.2021.3133430.

[35]. D. -R. Emenonye, C. Dietrich and R. M. Buehrer, "Differential Modulation in Massive MIMO With Low-Resolution ADCs," in *IEEE Transactions on Wireless Communications*, vol. 21, no. 6, pp. 4482-4496, June 2022, doi: 10.1109/TWC.2021.3130499.

[36]. Osama, Islam; Rihan, Mohamed; Elhefnawy, Mohamed; Eldolil, Sami; Malhat, Hend Abd El-Azem,"A Review on Precoding Techniques for mm-Wave Massive MIMO Wireless Systems", International Journal of Communication Networks and Information Security; Kohat Vol. 14, Iss. 1, (Apr 2022): 26-36.

[37]. L. Wen, H. Qian, Y. Hu, Z. Deng and X. Luo, "One-bit Downlink Precoding for Massive MIMO OFDM System," in IEEE Transactions on Wireless Communications, 2023, doi: 10.1109/TWC.2023.3238380.

[38]. Wence Zhang, Jing Xia, Xu Bao, "Massive MIMO Systems with Low-Resolution ADCs: Achievable Rates and Allocation of Quantization Bits", Wireless Communications and Mobile Computing, vol. 2023, Article ID 4012841, 12 pages, 2023. https://doi.org/10.1155/2023/4012841.